Fractalkine Preferentially Mediates Arrest and Migration of CD16$^+$ Monocytes

Petronela Ancuta,[1] Ravi Rao,[2] Ashlee Moses,[3] Andrew Mehle,[1] Sunil K. Shaw,[2] F. William Luscinskas,[2] and Dana Gabuzda[1]

[1]*Department of Cancer Immunology and AIDS, Dana-Farber Cancer Institute, and* [2]*Department of Pathology, Brigham and Women's Hospital, Harvard Medical School, Boston, MA 02115*

[3]*Vaccine and Gene Therapy Institute, Oregon Health & Sciences University, Beaverton, OR 97006*

Abstract

CD16$^+$ monocytes represent 5–10% of peripheral blood monocytes in normal individuals and are dramatically expanded in several pathological conditions including sepsis, human immunodeficiency virus 1 infection, and cancer. CD16$^+$ monocytes produce high levels of proinflammatory cytokines and may represent dendritic cell precursors in vivo. The mechanisms that mediate the recruitment of CD16$^+$ monocytes into tissues remain unknown. Here we investigate molecular mechanisms of CD16$^+$ monocyte trafficking and show that migration of CD16$^+$ and CD16$^-$ monocytes is mediated by distinct combinations of adhesion molecules and chemokine receptors. In contrast to CD16$^-$ monocytes, CD16$^+$ monocytes expressed high CX3CR1 and CXCR4 but low CCR2 and CD62L levels and underwent efficient transendothelial migration in response to fractalkine (FKN; FKN/CX3CL1) and stromal-derived factor 1α (CXCL12) but not monocyte chemoattractant protein 1 (CCL2). CD16$^+$ monocytes arrested on cell surface–expressed FKN under flow with higher frequency compared with CD16$^-$ monocytes. These results demonstrate that FKN preferentially mediates arrest and migration of CD16$^+$ monocytes and suggest that recruitment of this proinflammatory monocyte subset to vessel walls via the CX3CR1-FKN pathway may contribute to vascular and tissue injury during pathological conditions.

Key words: chemokines • chemokine receptors • chemotaxis • cell adhesion • inflammation

Introduction

Peripheral blood monocytes are a heterogeneous population (for review see 1). In normal individuals, 90–95% of circulating monocytes express high CD14 and CD64 (FcγRI) levels, whereas 5–10% express CD16 (FcγRIII; for review see 2). Two subsets of CD16$^+$ monocytes can be distinguished: CD14^{high} CD64$^+$ and CD14^{low} CD64$^-$ (1). A dramatic increase in circulating CD16$^+$ monocytes has been reported in pathologies such as sepsis, HIV-1 infection, metastatic cancer, tuberculosis, and asthma (2–4). Compared with CD16$^-$ monocytes, CD16$^+$ monocytes produce higher levels of TNF-α (3, 5) and IL-1 (3) but not IL-10 (2), exhibit lower phagocytic activity (1), and have higher antigen presenting capacity (1). A recent report demonstrated that CD16$^+$ monocytes preferentially differentiate into dendritic cells in a model of transendothelial trafficking (6), suggesting that CD16$^+$ monocytes represent dendritic cell precursors in vivo.

Although several reports have documented functional characteristics of CD16$^+$ monocytes (1–6), the mechanisms of CD16$^+$ monocyte recruitment into tissues remain unknown. Monocyte chemoattractant protein 1 (MCP-1;* CCL2), the most potent chemokine for CD16$^-$ monocytes, does not trigger transendothelial migration (TEM) of CD16$^+$ monocytes as a consequence of low CCR2 expression (7). Furthermore, L-selectin (CD62L), which mediates lymphocyte homing into lymph nodes (8), is expressed at

The online version of this article contains supplemental material.

Address correspondence to Dana Gabuzda, Department of Cancer Immunology and AIDS, Dana-Farber Cancer Institute, Harvard Medical School, 44 Binney Street, JFB 816, Boston, MA 02115. Phone: 617-632-2154; Fax: 617-632-3113; E-mail: dana_gabuzda@dfci.harvard.edu

*Abbreviations used in this paper: FKN, fractalkine; HUVEC, human umbilical vascular endothelial cells; ICAM-1, intercellular adhesion molecule 1; iHUVEC, immortalized HUVEC; IM, index of migration; MCP-1, monocyte chemoattractant protein 1; MIP-1α, macrophage inflammatory protein 1α; pHUVEC, primary HUVEC; PSGL-1, P-selectin glycoprotein ligand 1; SDF-1α, stromal-derived factor 1α; TEM, transendothelial migration; VCAM-1, vascular cell adhesion molecule 1; VLA-4, very late antigen 4.

high levels on $CD16^-$ monocytes but at very low levels on $CD16^+$ monocytes (9), raising the possibility that $CD16^+$ monocytes may not be recruited into lymph nodes. Whether $CD16^+$ monocytes are recruited into nonlymphoid tissues via chemokines other than MCP-1 is unknown. Recent studies demonstrate that distinct chemokines trigger migration of specific monocyte subsets (for review see 10). MCP-1 mediates $CCR2^+$ $CD62L^+$ monocyte recruitment into lymph nodes under inflammatory conditions (11), constitutive breast- and kidney-expressed chemokine (BRAK/CXCL14) is selectively chemotactic for prostaglandin E2–stimulated monocytes (12), and monokine induced by IFN-γ (MIG/CXCL9) mediates recruitment of a minor $CXCR3^+$ monocyte subset (13). These findings suggest distinct mechanisms for tissue-specific recruitment of monocyte subsets similar to those described for lymphocytes (14).

Given the dramatic expansion of $CD16^+$ monocytes in several pathological conditions, we sought to characterize the mechanism of their recruitment into tissues. Here we demonstrate that $CD16^-$ and $CD16^+$ monocytes have distinct patterns of chemotactic migration and that fractalkine (FKN; FKN/CX3CL1) plays a key role in mediating preferential arrest and migration of $CD16^+$ monocytes. These results suggest that proinflammatory $CD16^+$ monocytes might be preferentially recruited into anatomic sites expressing FKN and contribute to vascular and tissue injury during pathological conditions in which this monocyte subset is expanded.

Materials and Methods

Reagents and Antibodies. Recombinant human MCP-1, macrophage inflammatory protein 1α (MIP-1α), stromal-derived factor 1α (SDF-1α), FKN, TNF-α, and IFN-γ were from R&D Systems. FKN biotin was from Exalpha Biologicals Inc. The following antibodies were used: FITC anti-CD14, anti-CD16, anti-CD16b, anti-CD62L, PE anti-CD33, CD56, anti–intercellular adhesion molecule 1 (ICAM-1), and PC5 anti-CD16 mAbs (Beckman Coulter); FITC anti-CD62E and PE anti-CCR1, anti-CCR2, anti-CCR3, anti-CXCR5, and anti-FKN mAbs (R&D Systems); FITC anti-CX3CR1 mAb (MBL International Corporation); FITC anti-CD3, anti-CD32, anti-CD64, PE anti-CCR5, anti-CXCR1, anti-CXCR2, anti-CXCR4, anti–P-selectin glycoprotein ligand 1 (PSGL-1), anti-CD18, anti-CD11a, anti-CD11b, anti-CD11c, anti-CD49d, anti–HLA-DR, and anti–vascular cell adhesion molecule 1 (VCAM-1) mAbs (BD Biosciences).

Cell Isolation. PBMCs were isolated from fresh blood of healthy volunteers by Ficoll-Paque gradient centrifugation. The study protocol and informed consent forms were approved by the Dana-Farber Cancer Institute Institutional Review Board. Monocytes were isolated by negative selection using magnetic beads (Miltenyi Biotec). The purity of the monocyte fraction was 95–98% as determined by staining with anti-CD14, anti-CD33, anti-CD16b, and anti-CD56 mAbs and FACS® analysis. $CD16^-$ and $CD16^+$ monocyte subsets were then isolated using magnetic beads coated with anti-CD16 mAb (Miltenyi Biotec). Staining with anti-CD14 and anti-CD16 mAbs showed >95% $CD16^-$ monocytes in the $CD16^-$ fraction and >80% $CD16^+$ monocytes in the $CD16^+$ fraction.

FKN Binding. Monocytes from whole blood and PBMCs were stained with PE anti-CD33, PC5 anti-CD16 mAbs, and FKN biotin (extracellular domain, 0.5 μg/10^6 cells for 30 min at 4°C) followed by FITC streptavidin. The specificity of FKN binding was determined by preincubation of the cells with unlabeled FKN (extracellular domain, 1 μg/10^6 cells for 10 min at 4°C). Fixed cells were then subjected to FACS® analysis.

RT-PCR Detection of CX3CR1 mRNA. Total RNA was isolated using the RNeasy mini kit (QIAGEN), primed (1 μg) with random hexamers (Promega), and reverse transcribed. Limiting dilutions of cDNA from the RT reaction mixture were subjected to PCR amplification using Taq polymerase (Invitrogen) for 35 cycles (94°C for 30 s, 58°C for 30 s, and 72°C for 1 min). The CX3CR1 primers were: 5′-ACT CGT CTC TGG TAA AGT CTG -3′ and 5′-GGC TTT GGC TTT CTT GTG G-3′. The β globin primers were: 5′-CAA CTT CAT CCA CGT TCA CC-3′ (PCO4) and 5′-GAA GAG CCA AGG ACA GGT AC-3′ (GH2O).

Endothelial Cell Immortalization and Culture. Primary human umbilical vascular endothelial cells (HUVEC) were purchased from Clonetics/BioWhittaker and immortalized with the recombinant retrovirus LXSN16 E6/E7 as previously described (15) to expand their lifespan in vitro. Immortalized HUVEC (iHUVEC) were cultured on collagen-coated flasks in EGM-MV medium (BioWhittaker) containing 200 μg/ml G418.

Immunofluorescence Staining. Primary HUVEC (pHUVEC) and iHUVEC were cultured at confluence on fibronectin-coated coverslips, fixed with ethanol at −20°C, and then stained with anti–JAM-1 (2A9; provided by C. Parkos, Emory University School of Medicine, Atlanta, GA), anti–β-catenin (Research Diagnostics), or anti–VE-cadherin mAbs (Beckman Coulter) as previously described (16).

Transwell and TEM Assays. Chemotaxis assays were performed as previously described (7, 17). In brief, iHUVEC were cultured on collagen-coated transwells (6.5 mm diameter and 5 μm pore size; Corning Costar) at 2×10^5 cells/well in EGM-MV medium for 2 d. The confluence of the monolayers was assessed by measurement of the electrical resistance using a Millicell®–ERS electrode (Millipore). Serial dilutions of chemokines in DMEM containing 0.5% BSA were placed in the bottom chamber of the transwell system. 10^6 monocytes isolated by negative selection and stained with PC5 anti-CD16 mAb were placed in the upper chamber and incubated for 2.5–4 h at 37°C. The number of migrated $CD16^-$ and $CD16^+$ monocytes was determined by FACS® analysis using Flow-Count Fluorospheres (Beckman Coulter). The index of migration (IM) was calculated as the ratio between the number of cells migrated in response to chemokine and medium alone.

Generation of FKN-expressing HUVEC Line. The FKN open reading frame was amplified via PCR from pORF9hFractalkine (InvivoGen), cloned into pcDNA3.1/Hygro(+) (Invitrogen), and confirmed by sequencing. pcDNA3.1/Hygro(+)/FKN was transfected into iHUVEC using Lipofectamine 2000 (Invitrogen). FKN-transfected iHUVEC were cultured in EGM-MV medium containing 200 μg/ml G418 and 100 μg/ml hygromycin and then sorted by FACS® for high membrane-bound FKN expression (FKN-HUVEC).

Adhesion Assay under Flow Conditions. The parallel flow chamber used in this study has been previously described (16, 18). Endothelial cells were cultured on fibronectin-coated coverslips and then assembled in the flow chamber. The chamber was mounted on a phase contrast/fluorescence microscope (Nikon Eclipse TE 300) connected to an Orca ER camera (Hamamatsu).

Images were acquired using MetaMorph software. Monocytes isolated by negative selection were stained with FITC anti-CD16 mAb, suspended at 10^6/ml, and perfused over the endothelial monolayers at a shear stress rate of 0.5 dynes/cm^2 using a syringe pump (Harvard Apparatus). The number of total and CD16$^+$ monocytes arrested onto endothelial cells was determined by counting five different microscope fields.

Online Supplemental Material. We use FACS® analysis to demonstrate comparable expression of E-selectin and ICAM-1 on TNF-α–stimulated pHUVEC and iHUVEC, and an in vitro flow model to demonstrate firm arrest of CD16$^+$ monocytes onto TNF-α/IFN-γ–stimulated pHUVEC under flow. The online supplemental figures are available at http://www.jem.org/cgi/content/full/jem.20022156/DC1.

Results and Discussion

CD16$^+$ Monocytes Express High Levels of CX3CR1. The expression of a large panel of chemokine receptors and adhesion molecules was assessed on monocyte subsets. Staining with anti-CD14 and anti-CD16 mAbs distinguished three monocyte subsets: CD14^{high} CD16$^-$, CD14^{high} CD16$^+$, and CD14^{low} CD16$^+$, representing 85.5 ± 6.2, 3.6 ± 1.5, and 6.7 ± 3.0% of total monocytes, respectively (mean ± SD, $n = 8$; Fig. 1 A), consistent with previous reports (1). The high expression of HLA-DR on CD14^{low} CD16$^+$ monocytes, together with the absence of neutrophil (CD16b, expressed on neutrophils but not monocytes nor NK cells; 19), NK (CD56), and T cell (CD3) markers (Fig. 1, B and D, and unpublished data), demonstrated the monocyte identity of these cells. The major CD14^{high} CD16$^-$ monocyte subset expressed high CCR1, CCR2, CXCR2, CXCR4, PSGL-1, CD62L, CD18, CD11a, CD11b, CD11c, very late antigen 4 (VLA-4), ICAM-1, CD31, CD44, CD32, CD64, and HLA-DR, intermediate CXCR1, and low or undetectable CCR3, CCR5, CXCR5, and CX3CR1 levels (Fig. 1, C and D, and unpublished data). Compared with CD16$^-$ monocytes, CD14^{low} CD16$^+$ monocytes expressed significantly lower levels of CCR1, CCR2, CXCR1, and CXCR2, similar levels of CXCR4, and higher levels of CX3CR1 (Fig. 1 C). The expression of PSGL-1 was high in both monocyte subsets, whereas CD62L expression was high on CD16$^-$ monocytes but low or undetectable on CD14^{low} CD16$^+$ monocytes (Fig. 1 D). The adhesion molecules CD18, CD11a, CD11b, CD11c, VLA-4, ICAM-1, CD31, and CD44 were expressed on 95–100% of both CD16$^-$ and CD14^{low} CD16$^+$ monocytes (Fig. 1 D and unpublished data). The mean fluorescence intensity for CD18, CD11a, CD11c, VLA-4, and CD31 expression was higher on CD16$^+$ monocytes as compared with CD16$^-$ monocytes (unpublished data). The phenotype of CD14^{high} CD16$^+$ monocytes was intermediate between that of CD14^{low} CD16$^+$ and CD16$^-$ monocytes (Fig. 1, C and D). Similar to CD14^{low} CD16$^+$ monocytes, a significant decrease in CCR2, CD62L, and CD64, and increase in CX3CR1 expression was observed on CD14^{high} CD16$^+$ compared with CD16$^-$ monocytes. CD14^{high} CD16$^+$ monocytes could be distinguished from the other two monocyte subsets by high CCR5 expression (Fig. 1 C).

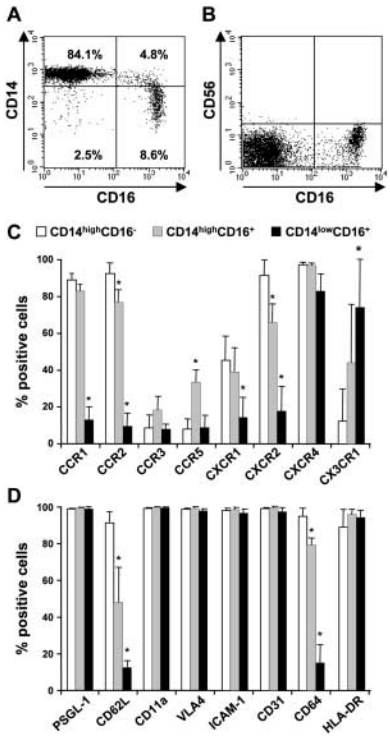

Figure 1. Phenotypic analysis of human monocyte subsets. (A) PBMCs were stained with FITC anti-CD14 and PC5 anti-CD16 mAbs. Monocytes were gated according to size, granularity, and CD14 expression. Three subsets of monocytes were identified: CD14^{high} CD16$^-$, CD14^{high} CD16$^+$, and CD14^{low} CD16$^+$. Results are representative of experiments performed with cells from 20 different donors. (B) PBMCs were stained with FITC anti-CD14, PE anti-CD56, and PC5 anti-CD16 mAbs, and CD14$^+$ monocytes were analyzed for CD16 and CD56 expression. Results are representative of four experiments performed with cells from different donors. (C and D) PBMCs were stained with FITC anti-CD14, PC5 anti-CD16, and the indicated mAbs, and the phenotype of each monocyte subset was analyzed by flow cytometry. Values represent the percentage of positive cells (mean ± SD, $n = 9$). *, $P < 0.05$, Student's t test (CD16$^+$ vs. CD16$^-$ monocytes).

The pattern of CCR1, CCR2, CX3CR1, and CD62L expression on the three monocyte subsets was similar when staining was performed on whole blood and PBMCs, indicating that expression of these markers was not altered by Ficoll separation (unpublished data).

We further analyzed the expression of CX3CR1 molecules by intracellular staining and observed high, intermediate, and low/undetectable levels of CX3CR1 expression in CD14^{low} CD16$^+$, CD14^{high} CD16$^+$, and CD14^{high} CD16$^-$ monocytes, respectively (unpublished data). Moreover, semiquantitative RT-PCR demonstrated that the level of CX3CR1 mRNA in CD16$^+$ monocytes was more than twofold higher compared with CD16$^-$ monocytes as determined by the CX3CR1/β globin mRNA ratio for an RT product dilution of 1:20 (Fig. 2). CX3CR1 is the receptor for FKN, a membrane-bound glycoprotein with a unique CX3C chemokine domain atop an extended mucin-like stalk that can be released from the cell surface by proteolysis (for review see 20). We investigated whether differential expression of CX3CR1 on monocyte subsets is associated

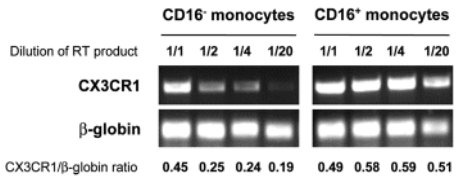

Figure 2. Expression of CX3CR1 mRNA in $CD16^-$ and $CD16^+$ monocytes. Total RNA from $CD16^-$ and $CD16^+$ monocytes was reverse transcribed and serial dilutions of the RT product were subjected to PCR amplification using CX3CR1 and β globin primers. The optical density of each PCR band was determined using Eagle Sight software (Stratagene). Results are representative of three experiments performed using monocytes from different donors.

with differences in their ability to bind FKN. Consistent with the levels of CX3CR1 expression, we detected low levels of FKN binding on $CD16^-$ monocytes, whereas $CD16^+$ monocytes, particularly $CD14^{low}$ $CD16^+$ monocytes from whole blood and PBMCs, specifically bound high levels of soluble FKN (Table I). FKN binding activity was previously demonstrated for NK cells, monocytes, and some $CD8^+$ T cells (17). Here we demonstrate that among circulating monocytes, high levels of CX3CR1 expression and FKN binding are detected on a minor $CD16^+$ subset, whereas $CD16^-$ monocytes exhibit very low CX3CR1 expression and little FKN binding. Similarly, two monocyte subsets have been identified in mouse, $CCR2^+$ $CX3CR1^{med}$ $CD62L^+$ and $CCR2^-$ $CX3CR1^{high}$ $CD62L^-$ (11), sharing phenotypic characteristics with human $CD16^-$ and $CD16^+$ monocytes, respectively. Human $CD16^+$ and mouse $CCR2^-$ $CX3CR1^{high}$ $CD62L^-$ monocytes do not migrate in response to MCP-1 (7, 11), but whether they are recruited by other chemokines is unknown.

FKN Triggers $CD16^+$ Monocyte Migration. The differential expression of chemokine receptors on monocyte subsets suggested that distinct mechanisms may regulate their trafficking. Thus, we investigated chemotactic migration of $CD16^-$ and $CD16^+$ monocytes in response to MCP-1, MIP-1α (CCL3), SDF-1α (CXCL12), and FKN. The expression of CD16 on monocytes rapidly decreases after several hours in culture (5 and unpublished data). Therefore, we stained monocytes with fluorescent anti-CD16 mAb and followed their chemotactic migration in a transwell system. Monocyte staining with anti-CD16 mAb had no significant effect on the total number of migrated cells (unpublished data). The spontaneous migration of $CD16^-$ monocytes was higher compared with that of $CD16^+$ monocytes (17.3 ± 3.4% vs. 9.5 ± 3.3%, mean ± SD, n = 3). In preliminary experiments, chemokine concentrations inducing optimal migration of monocytes were determined (e.g., 50–100 ng/ml for MCP-1, MIP-1α, and SDF-1α, and 1–10 ng/ml for FKN). The results presented in Fig. 3, A and C, demonstrate that $CD16^-$ and $CD16^+$ monocytes have distinct patterns of chemotactic migration. MCP-1, MIP-1α, and SDF-1α induced a high IM in $CD16^-$ monocytes, whereas a low IM was observed in response to FKN (Fig. 3 A). In contrast, $CD16^+$ monocytes did not migrate in response to MCP-1 nor MIP-1α but migrated efficiently in response to SDF-1α and FKN with a significantly higher IM (8.9 ± 0.1 and 5.7 ± 2.1, respectively) compared with $CD16^-$ monocytes (5.5 ± 1.2 and 2.1 ± 0.4, respectively; Fig. 3 A). Thus, consistent with high CX3CR1 and CXCR4 expression, $CD16^+$ monocytes underwent preferential migration in response to FKN and SDF-1α.

To emigrate from the vasculature, chemokine-activated leukocytes must penetrate between adjacent endothelial cells and gain access to the underlying basement membrane (21). Therefore, we investigated the ability of $CD16^-$ and $CD16^+$ monocytes to cross a confluent endothelial monolayer in response to MCP-1, SDF-1α, and FKN. For these studies we used iHUVEC, which formed confluent "cobblestone" monolayers and showed junctional staining for VE-cadherin, JAM1, β-catenin, and CD31 similar to pHUVEC (Fig. 3 B and unpublished data). Stimulation by TNF-α induced comparable levels of CD62E, ICAM-1, and VCAM-1 expression on iHUVEC and pHUVEC (Fig. S1, available at http://www.jem.org/cgi/content/full/jem.20022156/DC1, and unpublished data). The percentage of $CD16^-$ and $CD16^+$ monocytes that underwent spontaneous TEM (0.9 ± 0.2% and 0.3 ± 0.1%, respec-

Table I. *FKN Binding on Monocyte Subsets*

		Monocyte subsets		
		$CD14^{high}$ $CD16^-$	$CD14^{high}$ $CD16^+$	$CD14^{low}$ $CD16^+$
Blood	Percent positive cells	25.3 ± 10.1	30.0 ± 14.9	76.3 ± 4.7[a]
	MFI	15.5 ± 9.2	24.5 ± 13.4	31.0 ± 17.0
PBMC	Percent positive cells	29.0 ± 2.8	55.0 ± 8.5[a]	74.0 ± 15.6[a]
	MFI	14.1 ± 1.6	29.0 ± 1.0[a]	16.7 ± 2.4[a]

FKN binding was analyzed on monocyte subsets after staining of fresh blood and PBMCs from the same donor. Cells were incubated with FITC anti-CD14, PC5 anti-CD16, and FKN-biotin, and then with PE streptavidin. Values represent the percentage of cells binding FKN after subtracting the background (i.e., the level of FKN–biotin binding that was not blocked by preincubation with unlabeled FKN) and the geometric mean fluorescence intensity (mean ± SD, n = 3).
[a]$P < 0.05$, Student's t test ($CD16^+$ vs. $CD16^-$ monocytes).

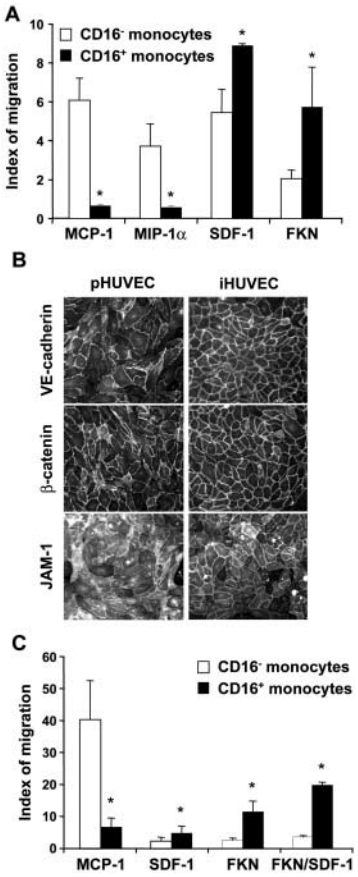

Figure 3. Chemotactic migration of $CD16^-$ and $CD16^+$ monocytes. (A) Monocytes were stained with PC5 anti-CD16 mAb and placed in the upper chamber of transwells. Chemokines were placed in the bottom chamber. After 2.5 h, $CD16^-$ and $CD16^+$ monocytes that migrated into the bottom chamber were counted by FACS®. The IM (mean ± SEM, n = 3–8) at optimal chemokine concentrations, 50 ng/ml for MCP-1, MIP-1α, and SDF-1α, and 10 ng/ml for FKN, is shown. (B) Confluent pHUVEC and iHUVEC monolayers were analyzed for junction expression of VE-cadherin, β-catenin, and JAM-1 molecules. Results are representative of two independent experiments. (C) Monocytes were assessed for their ability to cross a confluent iHUVEC monolayer in response to optimal concentrations of chemokines. After 4 h, $CD16^-$ and $CD16^+$ monocytes that migrated into the bottom chamber were counted by FACS®. The IM (mean ± SEM, n = 6) is shown. *, $P < 0.05$, Student's t test ($CD16^+$ vs. $CD16^-$ monocytes).

tively, mean ± SD, n = 3) was dramatically reduced compared with the transwell system, probably due to the strong adherence of monocytes to endothelial cells under static conditions (unpublished data). MCP-1 induced high TEM of $CD16^-$ monocytes (IM 40.3 ± 12.2), but low TEM of $CD16^+$ monocytes (6.9 ± 2.7, Fig. 3 C). The low TEM of $CD16^+$ monocytes in response to MCP-1 probably reflects migration of the $CD14^{high}$ $CD16^+$ subset, which expresses intermediate levels of CCR2. Consistent with the levels of CX3CR1 expression, FKN induced high TEM of $CD16^+$ monocytes (IM 11.5 ± 3.3), but little migration of $CD16^-$ monocytes (IM 2.7 ± 0.6, Fig. 3 C). $CD16^+$ monocytes underwent TEM with a significantly higher IM in response to FKN than to MCP-1 (11.5 ± 3.3 vs. 6.9 ± 2.7, $P < 0.05$; Fig. 3 C). Moreover, FKN in combination with SDF-1α dramatically increased the TEM of $CD16^+$ monocytes (IM 19.9. ± 0.8), but not $CD16^-$ monocytes (IM 3.8 ± 0.4, Fig. 3 C). These results suggest that FKN and SDF-1α, which are expressed under both constitutive and inflammatory conditions in vivo (20, 22), may act in an additive manner to regulate $CD16^+$ monocyte trafficking. The TEM of $CD16^+$ monocytes in response to FKN was lower compared with that of $CD16^-$ monocytes in response to MCP-1 (11.5 ± 3.3 vs. 40.3 ± 12.2, $P < 0.05$; Fig. 3 C). This difference in efficiency of TEM might be a consequence of the stronger adherence of $CD16^+$ monocytes to endothelial cells compared with that of $CD16^-$ monocytes (unpublished data). Previous studies reported the chemotactic effect of FKN on total monocytes (17, 23). In this study we demonstrate that FKN preferentially triggers migration of $CD16^+$ monocytes.

FKN Mediates Firm Arrest of $CD16^+$ Monocytes Under Flow. Monocyte recruitment into tissues requires sequential and overlapping adhesion pathways including CD62L, PSGL-1, VCAM-1, VLA-4, β2 integrins, ICAM-1, and CD31, and takes place under flow conditions (18, 24). Consistent with previous studies (9), we detected low expression of CD62L on $CD16^+$ monocytes, which may impair their ability to migrate into lymph nodes, as previously demonstrated for mouse $CCR2^-$ $CD62L^-$ monocytes (11). Whether $CD16^+$ monocytes are recruited into other peripheral tissues is unknown. The preceding experiments demonstrated that CX3CR1 is highly expressed on $CD16^+$ monocytes (Fig. 1 C and Table I) and that FKN induces preferential migration of these cells (Fig. 3, A and C). The membrane-bound form of FKN is expressed on endothelial cells after stimulation with inflammatory cytokines (23) and mediates monocyte adhesion under flow conditions (25). Thus, CX3CR1 might compensate for the low expression of CD62L on $CD16^+$ monocytes and thereby may play a critical role in recruitment of this monocyte subset. Therefore, we investigated the adhesion of $CD16^-$ and $CD16^+$ monocytes to FKN-expressing endothelial cells using an in vitro flow model. Optimal FKN expression was induced by stimulation of iHUVEC with TNF-α and IFN-γ (ST-HUVEC), which also induced high levels of CD62E and VCAM-1 expression (Fig. 4 A, top). A stable cell line (FKN-HUVEC) that expresses membrane-bound FKN in the absence of CD62E and VCAM-1 was generated (Fig. 4 A, bottom). Monocytes were perfused over endothelial monolayers at a flow rate of 0.5 dynes/cm^2. Under these conditions, monocytes attached to FKN-HUVEC and ST-HUVEC, but not to unstimulated HUVEC (Fig. 4 B, NS-HUVEC). The percentage of $CD16^+$ monocytes in the fraction arrested onto FKN-HUVEC was 2.6-fold higher than that in the input fraction (18.6 ± 3.4% vs. 7 ± 1.3%), indicating a more efficient interaction of $CD16^+$ monocytes with membrane-bound FKN compared with $CD16^-$ monocytes (Fig. 4 C). The percentage of $CD16^+$ monocytes arrested onto ST-HUVEC was slightly higher than that in the input fraction (8.6 ± 0.3% vs. 7.1 ± 1.3%;

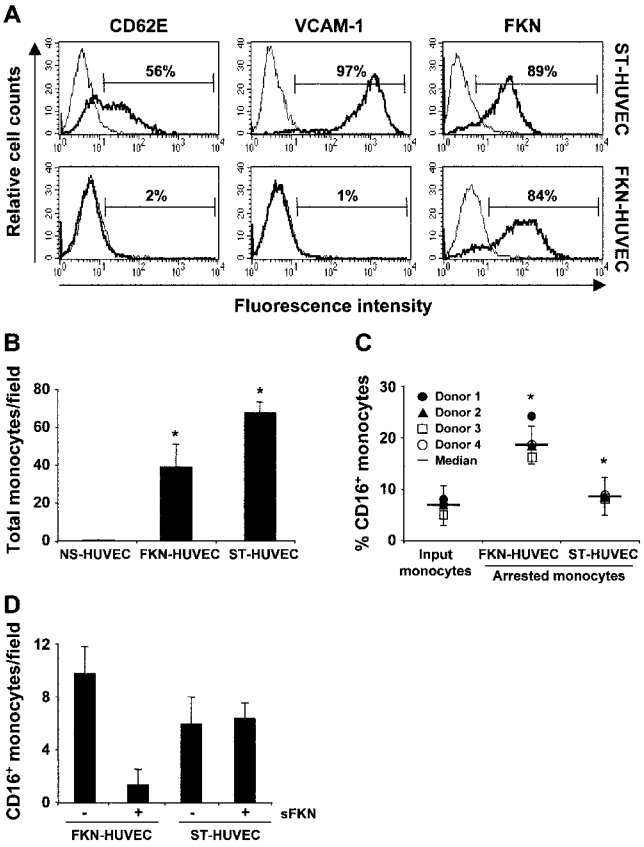

Figure 4. Firm arrest of CD16$^+$ monocytes onto endothelial cells under flow. (A) iHUVEC were incubated with 40 ng/ml TNF-α and 50 ng/ml IFN-γ (ST-HUVEC) for 5 h (top) or transfected to stably express FKN (bottom, KN-HUVEC). Cells were harvested, stained with anti-CD62E, anti–VCAM-1, and anti-FKN mAbs, and analyzed by FACS®. Results are representative of three independent experiments. (B) Monocytes were labeled with FITC anti-CD16 mAb and perfused over unstimulated (NS-HUVEC), ST-HUVEC, and FKN-HUVEC monolayers at 0.5 dynes/cm^2 flow rate. The number of total monocytes arrested onto endothelial cells (mean ± SD, $n = 4$) is shown. *, $P < 0.05$, Student's t test (FKN-HUVEC or ST-HUVEC vs. NS-HUVEC). (C) The percentage of CD16$^+$ monocytes in the input fraction was compared with that in the fraction arrested onto FKN-HUVEC and ST-HUVEC (mean ± SD, $n = 4$). *, $P < 0.05$, Student's t test (arrested vs. input fraction). (D) Monocytes were incubated with soluble FKN (1 μg/10^6 cells for 10 min at 4°C) and perfused over FKN-HUVEC and ST-HUVEC. Results are representative of two experiments performed with monocytes from different donors.

Fig. 4 C). Similar results were obtained when monocytes were perfused over TNF-α/IFN-γ–stimulated pHUVEC (Fig. S2, available at http://www.jem.org/cgi/content/full/jem.20022156/DC1). These results demonstrate that CD16$^+$ and CD16$^-$ monocytes attach to cytokine-stimulated HUVEC with similar efficiency despite different levels of CD62L expression and suggest that CX3CR1 preferentially mediates CD16$^+$ monocyte attachment to FKN-expressing endothelial cells.

We further sought to determine whether the CX3CR1 interaction with FKN is required for CD16$^+$ monocyte adhesion to endothelial cells. When monocytes were preincubated with soluble FKN, there was a dramatic decrease in the number of CD16$^+$ monocytes arrested onto FKN-HUVEC, but not ST-HUVEC (Fig. 4 D). Thus, CX3CR1 is not the only molecule involved in CD16$^+$ monocyte recruitment onto inflamed endothelia. Other adhesion molecules might compensate for the low expression of CD62L and contribute to the accumulation of CD16$^+$ monocyte onto endothelial cells. For example, PSGL-1, which is highly expressed on CD16$^+$ monocytes, may interact with CD62E expressed on cytokine-stimulated endothelial cells (Fig. 4 A, top; reference 18) and thereby mediate CD16$^+$ monocyte arrest. The demonstration that CD16$^+$ monocytes can arrest onto endothelial cells in the presence of soluble FKN is consistent with previous reports demonstrating unaltered monocyte trafficking in CX3CR1- and FKN-deficient mice (26, 27). Nevertheless, recent studies indicate that FKN-mediated monocyte infiltration plays a critical role in atherosclerotic plaque formation (28, 29), suggesting that monocyte recruitment via the CX3CR1-FKN pathway can have deleterious consequences in vivo.

In summary, we identified FKN as the major chemokine and adhesion molecule mediating CD16$^+$ monocyte arrest and migration. FKN alone or in combination with SDF-1α preferentially triggered TEM of CD16$^+$ monocytes. In contrast, MCP-1 and MIP-1α were potent chemokines for CD16$^-$ but not CD16$^+$ monocytes. Consistent with their high CX3CR1 expression, CD16$^+$ monocytes arrested on cell surface–expressed FKN under flow with higher frequency compared with CD16$^-$ monocytes. These findings suggest that CD16$^+$ monocytes might be preferentially recruited into anatomic sites expressing FKN. Taking into account our results and those recently reported by other groups (28, 29), we propose that CD16$^+$ monocytes might be preferentially recruited to the vessel wall via locally expressed FKN and play an important role in atherosclerotic lesion formation. Furthermore, CD16$^+$ monocytes might be recruited into the brain of AIDS patients expressing high levels of FKN and SDF-1 (22, 30), and mediate blood-brain barrier damage and neuronal injury in HIV-associated dementia via their release of proinflammatory cytokines (3, 5) and neurotoxic factors (4). Understanding mechanisms of CD16$^+$ monocyte trafficking and the functional role of these cells in pathological conditions may suggest new therapeutic strategies to prevent deleterious consequences of monocyte infiltration to sites of chronic inflammation.

We thank L.J. Morse, J. Wang, T. Betz, and M. McPike for excellent technical assistance and helpful discussions.

This work was supported by National Institutes of Health (NIH) grants NS37277 and DA16549 to D. Gabuzda, HL36028, HL53993, HL56985, and HL65090 to F.W. Luscinskas, and NIH KO1 DK02798 to S.K. Shaw. Core facilities were supported by a Center for AIDS Research grant (AI2869) and the DFCI/Harvard Cancer Center. A. Mehle was supported in part by a National Science Foundation predoctoral fellowship and R. Rao by an Arthritis Research Campaign Traveling Fellowship. D. Gabuzda is an Elizabeth Glaser Scientist supported by the Pediatric AIDS Foundation.

Submitted: 17 December 2002
Revised: 20 April 2003
Accepted: 20 April 2003

References

1. Grage-Griebenow, E., H.D. Flad, and M. Ernst. 2001. Heterogeneity of human peripheral blood monocyte subsets. *J. Leukoc. Biol.* 69:11–20.
2. Ziegler-Heitbrock, H.W. 1996. Heterogeneity of human blood monocytes: the $CD14^+CD16^+$ subpopulation. *Immunol. Today.* 17:424–428.
3. Thieblemont, N., L. Weiss, H.M. Sadeghi, C. Estcourt, and N. Haeffner-Cavaillon. 1995. $CD14^{low}CD16^{high}$: a cytokine-producing monocyte subset which expands during human immunodeficiency virus infection. *Eur. J. Immunol.* 25:3418–3424.
4. Pulliam, L., R. Gascon, M. Stubblebine, D. McGuire, and M.S. McGrath. 1997. Unique monocyte subset in patients with AIDS dementia. *Lancet.* 349:692–695.
5. Belge, K.U., F. Dayyani, A. Horelt, M. Siedlar, M. Frankenberger, B. Frankenberger, T. Espevik, and L. Ziegler-Heitbrock. 2002. The proinflammatory $CD14^+CD16^+DR^{++}$ monocytes are a major source of TNF. *J. Immunol.* 168: 3536–3542.
6. Randolph, G.J., G. Sanchez-Schmitz, R.M. Liebman, and K. Schakel. 2002. The $CD16^+$ ($Fc\gamma RIII^+$) subset of human monocytes preferentially becomes migratory dendritic cells in a model tissue setting. *J. Exp. Med.* 196:517–527.
7. Weber, C., K.U. Belge, P. von Hundelshausen, G. Draude, B. Steppich, M. Mack, M. Frankenberger, K.S. Weber, and H.W. Ziegler-Heitbrock. 2000. Differential chemokine receptor expression and function in human monocyte subpopulations. *J. Leukoc. Biol.* 67:699–704.
8. Kishimoto, T.K., M.A. Jutila, and E.C. Butcher. 1990. Identification of a human peripheral lymph node homing receptor: a rapidly down-regulated adhesion molecule. *Proc. Natl. Acad. Sci. USA.* 87:2244–2248.
9. Steppich, B., F. Dayyani, R. Gruber, R. Lorenz, M. Mack, and H.W. Ziegler-Heitbrock. 2000. Selective mobilization of $CD14^+CD16^+$ monocytes by exercise. *Am. J. Physiol. Cell Physiol.* 279:C578–C586.
10. Muller, W.A. 2001. New mechanisms and pathways for monocyte recruitment. *J. Exp. Med.* 194:47–51.
11. Palframan, R.T., S. Jung, G. Cheng, W. Weninger, Y. Luo, M. Dorf, D.R. Littman, B.J. Rollins, H. Zweerink, A. Rot, et al. 2001. Inflammatory chemokine transport and presentation in HEV: a remote control mechanism for monocyte recruitment to lymph nodes in inflamed tissues. *J. Exp. Med.* 194:1361–1373.
12. Kurth, I., K. Willimann, P. Schaerli, T. Hunziker, I. Clark-Lewis, and B. Moser. 2001. Monocyte selectivity and tissue localization suggests a role for breast and kidney-expressed chemokine (BRAK) in macrophage development. *J. Exp. Med.* 194:855–861.
13. Janatpour, M.J., S. Hudak, M. Sathe, J.D. Sedgwick, and L.M. McEvoy. 2001. Tumor necrosis factor–dependent segmental control of MIG expression by high endothelial venules in inflamed lymph nodes regulates monocyte recruitment. *J. Exp. Med.* 194:1375–1384.
14. Kunkel, E.J., and E.C. Butcher. 2002. Chemokines and the tissue-specific migration of lymphocytes. *Immunity.* 16:1–4.
15. Moses, A.V., K.N. Fish, R. Ruhl, P.P. Smith, J.G. Strussenberg, L. Zhu, B. Chandran, and J.A. Nelson. 1999. Long-term infection and transformation of dermal microvascular endothelial cells by human herpes virus 8. *J. Virol.* 73:6892–6902.
16. Shaw, S.K., B.N. Perkins, Y.C. Lim, Y. Liu, A. Nusrat, F.J. Schnell, C.A. Parkos, and F.W. Luscinskas. 2001. Reduced expression of junctional adhesion molecule and platelet/endothelial cell adhesion molecule-1 (CD31) at human vascular endothelial junctions by cytokines tumor necrosis factor-alpha plus interferon-gamma does not reduce leukocyte transmigration under flow. *Am. J. Pathol.* 159:2281–2291.
17. Imai, T., K. Hieshima, C. Haskell, M. Baba, M. Nagira, M. Nishimura, M. Kakizaki, S. Takagi, H. Nomiyama, T.J. Schall, et al. 1997. Identification and molecular characterization of fractalkine receptor CX3CR1, which mediates both leukocyte migration and adhesion. *Cell.* 91:521–530.
18. Luscinskas, F.W., H. Ding, P. Tan, D. Cumming, T.F. Tedder, and M.E. Gerritsen. 1996. L- and P-selectins, but not CD49d (VLA-4) integrins, mediate monocyte initial attachment to TNF-α-activated vascular endothelium under flow *in vitro*. *J. Immunol.* 157:326–335.
19. Perussia, B., and J.V. Ravetch. 1991. $Fc\gamma RIII$ (CD16) on human macrophages is a functional product of the $Fc\gamma RIII$-2 gene. *Eur. J. Immunol.* 21:425–429.
20. Umehara, H., E. Bloom, T. Okazaki, N. Domae, and T. Imai. 2001. Fractalkine and vascular injury. *Trends Immunol.* 22:602–607.
21. Kubes, P. 2002. Introduction: the complexities of leukocyte recruitment. *Semin. Immunol.* 14:65–72.
22. Langford, D., V.J. Sanders, M. Mallory, M. Kaul, and E. Masliah. 2002. Expression of stromal cell-derived factor-1α protein in HIV encephalitis. *J. Neuroimmunol.* 127:115–126.
23. Bazan, J.F., K.B. Bacon, G. Hardiman, W. Wang, K. Soo, D. Rossi, D.R. Greaves, A. Zlotnik, and T.J. Schall. 1997. A new class of membrane-bound chemokine with a CX3C motif. *Nature.* 385:640–644.
24. Luscinskas, F.W., Y.C. Lim, and A.H. Lichtman. 2001. Wall shear stress: the missing step for T cell transmigration? *Nat. Immunol.* 2:478–480.
25. Fong, A.M., L.A. Robinson, D.A. Steeber, T.F. Tedder, O. Yoshie, T. Imai, and D.D. Patel. 1998. Fractalkine and CX3CR1 mediate a novel mechanism of leukocyte capture, firm adhesion, and activation under physiologic flow. *J. Exp. Med.* 188:1413–1419.
26. Jung, S., J. Aliberti, P. Graemmel, M.J. Sunshine, G.W. Kreutzberg, A. Sher, and D.R. Littman. 2000. Analysis of fractalkine receptor CX3CR1 function by targeted deletion and green fluorescent protein reporter gene insertion. *Mol. Cell. Biol.* 20:4106–4114.
27. Cook, D.N., S.C. Chen, L.M. Sullivan, D.J. Manfra, M.T. Wiekowski, D.M. Prosser, G. Vassileva, and S.A. Lira. 2001. Generation and analysis of mice lacking the chemokine fractalkine. *Mol. Cell. Biol.* 21:3159–3165.
28. Lesnik, P., C.A. Haskell, and I.F. Charo. 2003. Decreased atherosclerosis in $CX3CR1^{-/-}$ mice reveals a role for fractalkine in atherogenesis. *J. Clin. Invest.* 111:333–340.
29. Combadiere, C., S. Potteaux, J.L. Gao, B. Esposito, S. Casanova, E.J. Lee, P. Debre, A. Tedgui, P.M. Murphy, and Z. Mallat. 2003. Decreased atherosclerotic lesion formation in CX3CR1/apolipoprotein E double knockout mice. *Circulation.* 107:1009–1016.
30. Pereira, C.F., J. Middel, G. Jansen, J. Verhoef, and H.S. Nottet. 2001. Enhanced expression of fractalkine in HIV-1 associated dementia. *J. Neuroimmunol.* 115:168–175.